J|A|C|S ARTICLES

Published on Web 05/11/2009

Auger Electron Spectroscopy as a Probe of the Solution of Aqueous Ions

Wandared Pokapanich,[†] Henrik Bergersen,[†] Ioana L. Bradeanu,[†] Ricardo R. T. Marinho,[†] Andreas Lindblad,[†] Sebastien Legendre,[†] Aldana Rosso,[†] Svante Svensson,[†] Olle Björneholm,[†] Maxim Tchaplyguine,[‡] Gunnar Öhrwall,*[,‡] Nikolai V. Kryzhevoi,[§] and Lorenz S. Cederbaum[§]

Department of Physics and Materials Science, Uppsala University, P.O. Box 530, SE-751 21 Uppsala, Sweden, MAX-lab, Lund University, P.O. Box 118, SE-221 00 Lund, Sweden, and Theoretische Chemie, Physikalisch-Chemisches Institut, Universität Heidelberg, Im Neuenheimer Feld 229, D-69120 Heidelberg, Germany

Received December 11, 2008; E-mail: gunnar.ohrwall@maxlab.lu.se

Abstract: Aqueous potassium chloride has been studied by synchrotron-radiation excited core-level photoelectron and Auger electron spectroscopy. In the Auger spectrum of the potassium ion, the main feature comprises the final states where two outer valence holes are localized on potassium. This spectrum exhibits also another feature at a higher kinetic energy which is related to final states where outer valence holes reside on different subunits. Through *ab initio* calculations for microsolvated clusters, these subunits have been assigned as potassium ions and the surrounding water molecules. The situation is more complicated in the Auger spectrum of the chloride anion. One-center and multicenter final states are present here as well but overlap energetically.

Introduction

Auger electron spectroscopy (AES) is a powerful technique for investigating matter. AES has been used extensively to characterize solid materials and gases, and recently the method has become more accessible for investigations of liquids.[1] In the Auger process an electron is emitted in the decay of a core vacancy, and the energy of this electron is analyzed. The Auger electron carries information on the energies of both the core ionized intermediate state and the doubly charged final state, thereby offering a direct probe of the electronic structure.

AES is a potentially interesting technique for studying solvated ions, since it is a local probe but still sensitive to the surrounding. In very weakly bound systems, such as rare gas clusters, the two-hole final states observed in the core−valence−valence (CVV) Auger spectrum are well localized at the core−hole sites.[2] This can be explained by the weak bonding between the rare gas atoms. For water clusters, where the interaction between the molecules is stronger, the CVV Auger spectrum has contributions both from final states that are localized on the ionized molecule and from final states that are delocalized over several centers. The kinetic energies of the delocalized states are higher than those of the localized states because the spatial separation between the holes weakens the electrostatic interaction between them.[3] The solvation of Cl^- was recently investigated using resonant Auger spectroscopy, probing charge-transfer-to-solvent (CTTS) excited states in aqueous chloride.[4] Clearly, excited states of the chloride ion are coupled strongly enough to the solvent to allow charge transfer during the core−hole lifetime. What we aim to study is the interaction between the populated states, which is what is probed by regular Auger spectroscopy.

In the present work, AES is used together with valence band photoelectron spectroscopy and X-ray photoelectron spectroscopy (XPS) to investigate the electronic structure of aqueous potassium chloride. The main focus in the present study lies in characterizing the final states of the solvated ions. We show that the main feature of the K^+ AES is due to localized final states, where a closed-shell rare-gas model can be applied satisfactorily. However, at a higher kinetic energy we also find a feature which we attribute to delocalized final states involving vacancies on both the potassium ion and surrounding water molecules. For the Cl^- ion, the situation is more complex, due to an energetic overlap of localized and delocalized final states.

We also present *ab initio* calculations of the respective Auger spectra of the KCl molecule and selected $KCl(H_2O)_n$ ($n = 1-3$, 6) clusters to interpret the experimental results. The calculations support the explanation for the features at higher kinetic energies with delocalized final states involving molecular orbitals of

[†] Department of Physics and Materials Science, Uppsala University.
[‡] MAX-lab, Lund University.
[§] Theoretische Chemie, Physikalisch-Chemisches Institut, Universität Heidelberg.

(1) Winter, B.; Hergenhahn, U.; Faubel, M.; Björneholm, O.; Hertel, I. V. *J. Chem. Phys.* **2007**, *127*, 094501.
(2) Lundwall, M.; Tchaplyguine, M.; Öhrwall, G.; Feifel, R.; Lindblad, A.; Lindgren, A.; Sorensen, S. L.; Svensson, S.; Björneholm, O. *Chem. Phys. Lett.* **2004**, *392*, 433.
(3) Öhrwall, G.; et al. *J. Chem. Phys.* **2005**, *123*, 054310.
(4) Winter, B.; Aziz, E. F.; Ottosson, N.; Faubel, M.; Kosugi, N.; Hertel, I. V. *J. Am. Chem. Soc.* **2008**, *130*, 7130.

10.1021/ja8096866 CCC: $40.75

neighboring water molecules, and give further insight into the interpretation of the Auger spectra.

Method

Aqueous potassium chloride was prepared by mixing KCl (purity ≥ 99.0%, Sigma Aldrich) with deionized water to obtain a concentration of 2.0 m. The experiments were performed at beamline I411 at the Swedish synchrotron radiation facility MAX-lab.[5,6] The spectra were recorded using a 10 μm liquid jet injected into a differentially pumped vacuum chamber. The propagation of the jet was perpendicular to the direction of the photon beam and the spectrometer. Typical working pressures were in the 10^{-5} mbar range in the differential pumping stage, far from the jet, and in the 10^{-6} mbar range in the analyzer chamber. The setup has been described in detail elsewhere.[7]

A Scienta R4000 electron spectrometer, mounted at 90° relative to the polarization plane of the radiation, was used for all measurements. For Cl^- 2p XPS and AES, a photon energy of 255 eV was used. For K^+ 2p XPS and AES, the photon energy was 340 eV. Water valence, Cl^- 3p and K^+ 3p photoelectron spectra were recorded with the photon energy 60 eV. The total experimental resolution, due to the photon bandwidth and the spectrometer, was 0.17 eV for both the Cl^- 2p and K^+ 2p XPS, while it was 0.06 eV for the valence region. For the Cl^- 2p and K^+ 2p AES, where the photon bandwidth is of no importance, the resolution was 0.25 eV.

Experimental Results

In this section, we present our results in several steps. First, we present the K^+ LMM Auger spectrum and identify transitions leading to its main feature. Then, we concentrate on a conspicuous feature at high kinetic energy of K^+ AES, which provides clear evidence for the existence of delocalized final states involving orbitals of the solvent. Finally, we discuss the LMM Auger spectrum of Cl^-. Photoelectron spectra, recorded to obtain core−hole binding energies of the Cl^- 2p and K^+ 2p levels, are presented in the Supporting Information.

Auger Electron Spectra. In Figure 1 the $L_{2,3}M_{2,3}M_{2,3}$ Auger spectrum of K^+ is shown. It is similar to the respective spectrum of solid KCl[8,9] and does not contain as much structure as that of gas-phase KCl.[8] For a free K^+ ion, the lowest lying final state configuration in the Auger process will have two holes in the 3p shell, giving rise to ^{1}S, ^{1}D, and ^{3}P states. As an initial step in the analysis, we have fitted the $L_{2,3}M_{2,3}M_{2,3}$ feature with two series of peaks corresponding to these final states, one for each of the $2p_{1/2}$ and $2p_{3/2}$ components. The intensities of the $2p_{1/2}$ lines were set to half of those for the $2p_{3/2}$ components. The applicability of this ratio is discussed below, but it is a defensible first guess in the absence of other information. The K 2p spin−orbit splitting was fixed to 2.81 eV, as obtained from the fitting of the photoelectron spectrum. The spectrum is plotted both on a kinetic energy scale (lower axis) and a double ionization potential scale (upper axis),

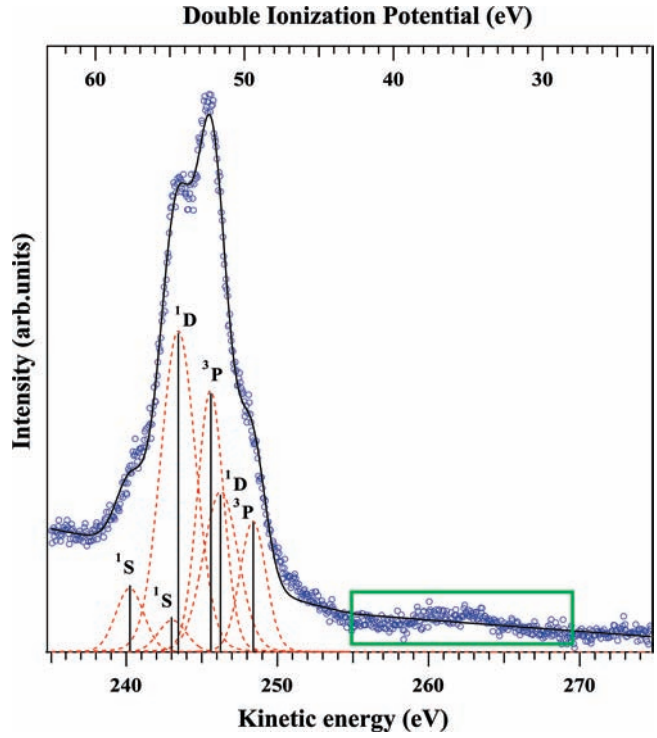

Figure 1. $L_{2,3}M_{2,3}M_{2,3}$ Auger spectrum of K^+ in aqueous KCl, corresponding to the transitions from the K^{+2} $2p^{-1}$ to the K^{+3} $3p^{-2}$ localized final state. The dashed lines show the individual fitted peaks. The solid line gives the resulting fit envelope. The solid vertical bars represent the center of gravity of the multiplet components. The feature at higher kinetic energy corresponds to the transitions from the K^{+2} $2p^{-1}$ to the K^{+2} $3p^{-1}$ + water valence vacancy final states (indicated by a rectangular frame). This part is expanded in Figure 2. The double ionization energy scale is referring to the $2p_{3/2}$ ionization.

Table 1. Experimental Kinetic Energies (Column A), Double Ionization Potentials (B), Relative Energies (C), and Relative Intensities (F) for the $L_3M_{2,3}M_{2,3}$ Auger spectra of Cl^- and K^+ in Aqueous KCl[a]

state	A (eV)	B (eV)	C (eV)	D (eV)	E (eV)	F (%)	G (%)
Cl ^{3}P	178.56	24.3	0	0	0	46	40
Cl ^{1}D	177.26	25.7	1.30	1.47	1.40	37	47
Cl ^{1}S	174.47	28.4	4.09	3.48	3.41	17	13
K ^{3}P	245.58	52.4	0	0	0	40	45
K ^{1}D	243.44	54.6	2.14	2.0	1.93	50	51
K ^{1}S	240.23	57.8	5.35	6.0	4.68	10	5

[a] The data are compared to experimental data for gas-phase KCl for Cl^- [17] and to solid KCl for K^+ [8] (relative energies, D; relative intensities, G), as well as data from NIST for Cl^+ and $K3^+$ ions[10] (relative energies, E).

the latter calculated as the difference in energy between the K $2p_{3/2}$ core−hole binding energy and the Auger kinetic energy. The energies and relative intensities obtained from the fitting are presented in Table 1, together with the experimental data for solid KCl,[9] as well as data from NIST for free K^{3+} ions (where a statistical average of the $^3P_{2,1,0}$ states have been used).[10]

The changes in binding energy and Auger kinetic energy upon solvation of potassium ions in liquid water have been estimated to $\Delta E_{BE}^{solv} = -8.54$ eV and $\Delta E_{AE}^{solv} = 12.41$ eV, respectively, using a statistical approach for the dominant Coulomb and polarization contributions.[11] The experimental value for the binding energy shift

(5) Bässler, M.; Forsell, J. O.; Björneholm, O.; Feifel, R.; Jurvansuu, M.; Aksela, S.; Sundin, S.; Sorensen, S. L.; Nyholm, R.; Ausmees, A.; Svensson, S. *J. Electron Spectrosc. Relat. Phenom.* **1999**, *101*−*103*, 953.
(6) Bässler, M.; Ausmees, A.; Jurvansuu, M.; Feifel, R.; Forsell, J. O.; Fonseca, P. T.; Kivimäki, A.; Sundin, S.; Sorensen, S. L.; Nyholm, R.; Björneholm, O.; Aksela, S.; Svensson, S. *Nucl. Instrum. Methods Phys. Res., Sect. A* **2001**, *469*, 382.
(7) Bergersen, H.; Marinho, R. R. T.; Pokapanich, W.; Lindblad, A.; Björneholm, O.; Sæthre, L. J.; Öhrwall, G. *J. Phys.: Condens. Matter* **2007**, *19*, 326101.
(8) Kukk, E.; Huttula, M.; Aksela, H.; Aksela, S.; Nõmmiste, E.; Kikas, A. *J. Phys. B* **2003**, *36*, L85.
(9) Elango, M.; Ruus, R.; Kikas, A.; Saar, A.; Ausmees, A.; Martinson, I. *Phys. Rev. B* **1996**, *53*, R5978.
(10) Ralchenko, Y.; Kramida, A. E.; Reader, J. *NIST Atomic Spectra Database,* version 3.1.5; NIST ASD Team, National Institute of Standards and Technology: Gaithersburg, MD, 2008.
(11) Ågren, H.; Siegbahn, H. *Chem. Phys.* **1985**, *95*, 37.

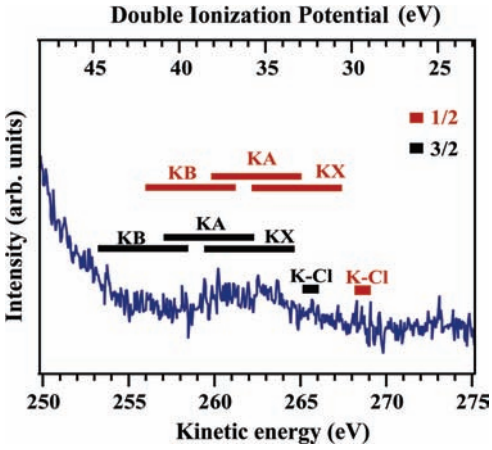

Figure 2. K^+ AES in aqueous KCl in the energy region corresponding to $K^{+2}\ 3p^{-1}$ + water valence vacancy final states. The horizontal solid lines show the estimated positions for the two-hole states KX, KA, KB, and K−Cl for both $2p_{3/2}$ (black) and $2p_{1/2}$ (red) (for explanation of notation, see text). The double ionization energy scale is referring to the $2p_{3/2}$ ionization.

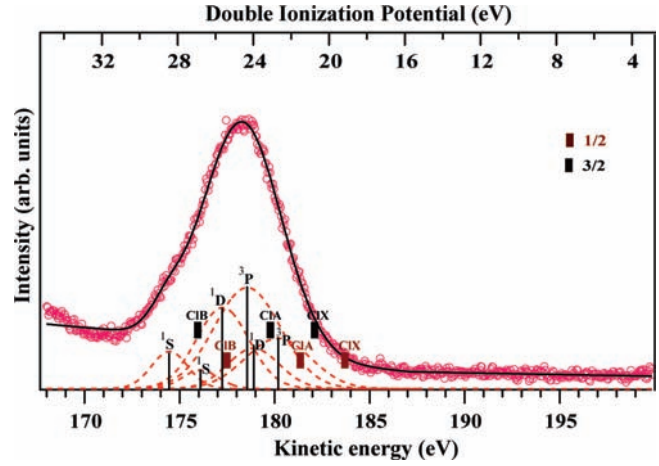

Figure 3. $L_{2,3}M_{2,3}M_{2,3}$ Auger spectrum of Cl^- in aqueous KCl, presented on a kinetic energy and a double ionization potential scale, the latter calculated as the difference in energy between the Cl^- $2p_{3/2}$ core−hole binding energy and the Auger kinetic energy. The dashed lines show the individual fitted peaks. The solid line gives the resulting fit envelope. The solid vertical thin lines represent the center of gravity of the multiplet components. The horizontal thick solid bars show the estimated positions for the two-hole states ClX, ClA, and ClB for both $2p_{3/2}$ (black) and $2p_{1/2}$ (red) (for explanation of notation, see text). The double ionization energy scale is referring to the $2p_{3/2}$ ionization.

of the K 3p level for a K^+ ion is 22.20 − 31.718 = −9.52 eV, using data from NIST for the free ion, with statistical average of the $^2P_{3/2,1/2}$ final states.[10] As far as we know, no data for the binding energy of the K 2p level of free potassium ions exist. With the assumption of the same binding energy shift for the K 2p and 3p levels, the change in Auger kinetic energy for the ^3P state upon solvation can be estimated as 77.535 − 52.4 − 9.428 = 15.71 eV, using data from NIST for the free ion, with a statistical average of the $^3P_{2,1,0}$ final states.[10] The agreement to our experimental data is reasonable, considering that quantum effects and the possible impact of the counterion are neglected in these calculations.[11]

Another conspicuous weak feature is present in the K^+ AES shown in Figure 1. It locates between 255 and 265 eV kinetic energy, i.e., ∼15−20 eV higher in energy than the main feature. The high kinetic energies suggest that this feature is caused by delocalized final states. In molecular KCl, a similar feature was found, but at ∼20−25 eV higher kinetic energy than the main feature. That feature was interpreted as arising from the transition from $K^{+2}\ 2p^{-1}$ to the ($K^{+2}\ 3p^{-1}$ + Cl $3p^{-1}$) delocalized final states.[8]

The energy of the final multicenter states can be estimated from the sum of the ionization energy of each of the involved valence electrons and the Coulomb repulsion between the vacant orbitals if the decay gives rise to spatially separated ions.[12] To be able to estimate the kinetic energies of Auger electrons from transitions to delocalized final states, we thus need the valence ionization energies of the species present in the sample. To this end, we have recorded a valence band photoelectron spectrum of the aqueous KCl solution. The recorded K^+ 3p line at 22.20 eV and Cl^- 3p line at 9.6 eV binding energies agree well with previous reported binding energies of solvated ions.[13] The liquid water X-state, A-state, and B-state binding energies agree with Winter et al., at 11.16, 13.50, and 17.34 eV, respectively.[14] From this we get the ionization energies for the valence levels. The Coulomb repulsion between the potassium ion and the ionized water molecules is more difficult to estimate. An upper bound can be found from the repulsion between two point charges, at the distance that corresponds to the equilibrium K^+−water distance in the liquid. The distance range is 2.73−2.81 Å,[15,16] which gives Coulomb repulsion of 5.12−5.27 eV. However, since the water valence levels are delocalized, the actual repulsion is likely to be smaller. The presence of a counterion in the vicinity would also lower the repulsion.

The high energy feature of Figure 1 is magnified in Figure 2 and shown together with estimated double ionization potentials for the final states with one vacancy on the potassium ion and one vacancy in the water valence orbitals. We use the notation KX, KA, and KB for these states indicating that after the decay water is in the singly ionized X-, A-, or B-state, respectively. We also show estimated two-hole binding energies for the final states with one vacancy on the K ion and one vacancy on the Cl ion. These states are marked by K−Cl. The energies of the KX, KA, and KB final states are shown as intervals, where the lowest binding energy end corresponds to no Coulomb repulsion, and the highest one to the Coulomb repulsion between point charges. The final states resulting from the decay of the initial K^+ ($2p_{3/2}$) vacancy are marked by black while the red color is used for the final states from the decay of the other spin orbit component. Figure 2 suggests that essentially all the intensity of the high kinetic energy feature in the K^+ Auger spectrum of the aqueous KCl solution arises due to the multicenter final states which involve the electrons of the potassium ion and the water environment. The calculations described below firmly support this supposition.

In Figure 3 the $L_{2,3}M_{2,3}M_{2,3}$ Auger spectrum of Cl^- is shown. In spite of the lack of sharp features, we have attempted to perform the same curve fit as for K^+ above, using the same assumptions. The energies and relative intensities obtained from this fitting procedure are presented in Table 1, together with comparisons to experimental data for the gas-phase molecule by Kivilompolo et al.,[17] as well as data from NIST.[10] Comparing the Cl^- AES for the aqueous KCl solution with the gas-phase[17] and the ionic solid phase spectra,[9] we find that the spectrum of the aqueous Cl^- is less resolved. This can partly be attributed to a greater variety in chemical surroundings in the relatively disordered liquid, compared to the gas phase and solid phase. We have used the same approach as for K^+ above to calculate the double ionization potentials for states with vacancies at Cl^- and water. With the notation ClX, ClA,

(12) Nordlund, D. Ph.D. Thesis, Physics Department, Stockholm University, Stockholm, Sweden, 2004.
(13) Weber, R.; Winter, B.; Schmidt, P. M.; Widdra, W.; Hertel, I. V.; Dittmar, M.; Faubel, M. *J. Phys. Chem. B* **2004**, *108*, 4729.
(14) Winter, B.; Weber, R.; Widdra, W.; Dittmar, M.; Faubel, M.; Hertel, I. V. *J. Phys. Chem. A* **2004**, *108*, 2625.
(15) Dang, L. X.; Schenter, G. K.; Glezakou, V. A.; Fulton, J. L. *J. Phys. Chem. B* **2006**, *110* (47), 23644.
(16) Ohtaki, H.; Fukushima, N. *J. Solution Chem.* **1992**, *21*, 23.
(17) Kivilompolo, M.; Kivimäki, A.; Aksela, H.; Huttula, M.; Aksela, S.; Fink, R. F. *J. Chem. Phys.* **2000**, *113*, 662.

and ClB to indicate that, after the decay, water is in the singly ionized X-, A-, or B-state, the energies of ClX, ClA, and ClB are found at 20.76, 23.10, and 26.94 eV, respectively. The final states resulting from the decay of the initial K^+ ($2p_{3/2}$) vacancy are marked by black while the red color is used for the final states resulted from the decay of the other spin orbit component. Note that in this case there is no Coulomb repulsion since the chloride final state is neutral. These energies mean that the delocalized final states energetically overlap with the main peak which has the double ionization potentials between ~18 and 34 eV. As will be discussed below, the energetic overlap leads to a redistribution of intensity between the localized and delocalized final states of the Auger decay, which will make the above analysis less appropriate.

As for K^+, the change in binding energy and Auger kinetic energy upon solvation of Cl^- ions in liquid water have been estimated using a statistical approach for the dominant electrostatic and polarization contributions, to $\Delta E_{BE}^{solv} = 4.55$ eV and $\Delta E_{AE}^{solv} = -0.85$ eV, respectively.[11] The experimental value for the binding energy shift of the Cl 3p level for a Cl^- ion is $9.6 - 3.667 = 5.9$ eV, using data from literature for the free ion, with statistical average of the $^2P_{3/2,1/2}$ final states.[10,18] As far as we know, no data for the binding energy of the Cl 2p level of free chloride ions exist. Assuming the same binding energy shift for the Cl 2p and 3p levels, the change in Auger kinetic energy for the ^3P state upon solvation can be estimated as $16.623 - 24.3 + 5.987 = -1.7$ eV, using data from literature for the free ion, with a statistical average of the $^3P_{2,1,0}$ final states.[10,18] Once again, the agreement between these estimates and our experimental data is reasonable.

Calculations

Computational Details. To interpret the experimental results in greater detail, we calculated Auger spectra of selected $KCl(H_2O)_n$ ($n = 1-3$, 6) clusters and of the KCl molecule. These small model systems provide sufficient information for elucidating the origin of the environmental features in the experimental Auger spectra. By considering these systems, we also gain insight into the dependence of the Auger spectra on the number and arrangement of water molecules and on the length of the K−Cl bond. We realize that certain aspects of bulk solvation, e.g., gas-to-liquid energy shifts, cannot be quantitatively predicted in the framework of microsolvation models of limited sizes. For these aspects, long-range interactions between the ionic compounds and solvent molecules much beyond the first solvation shell should be taken into account.

We used optimized geometries for all the systems except for the KCl molecule where the experimental equilibrium bond length of 2.67 Å was chosen. For the clusters with up to three water molecules the low energy conformers were considered, but the calculated spectra of only those of the global minimum are shown below. The geometries of these clusters are known in the literature (see ref 19) and represent structures composed of a *contact* K^+/Cl^- ion pair and the water molecules which are not bonded to each other by hydrogen bonds and play a role of bridges between the K^+ and Cl^- ions as shown in the respective insets of Figures 4 and 5. To clarify the impact of distinctive dissociation patterns of the KCl molecule on the Auger spectra a cluster containing a *solvent separated* K^+/Cl^- ion pair was also considered. A hexahydrated KCl cluster is expected to be the smallest cluster where the *solvent separated* K^+/Cl^- ion pair can be stabilized.[19] This is a cube-shaped cluster with a water hexamer which is composed of two interconnected three-membered rings placed between the counterions of the ionic KCl molecule (see the respective insets of Figures 4 and 5). For more details on the cluster geometries see Supporting Information.

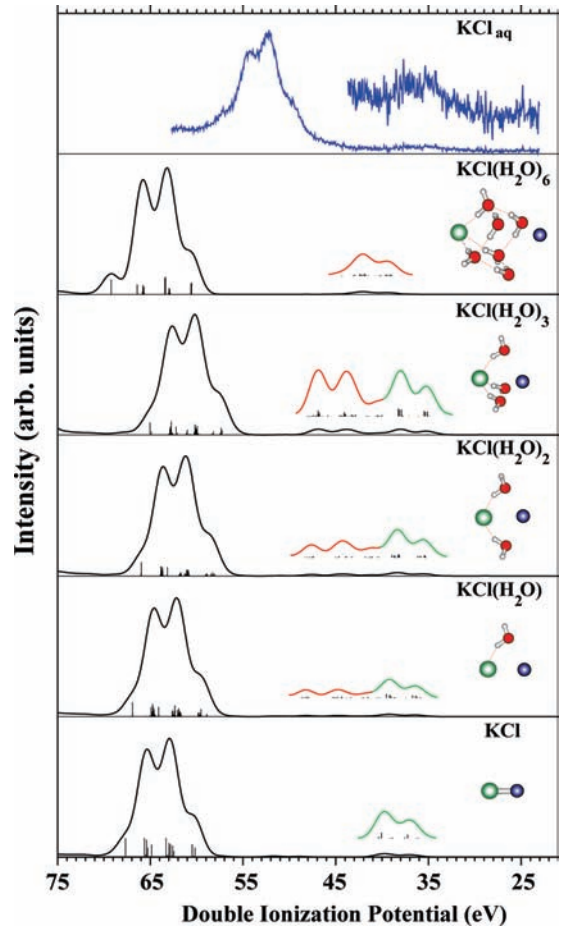

Figure 4. Comparison of the experimental K^+ Auger spectrum of aqueous KCl with the calculated spectra of the $KCl(H_2O)_{1-3,6}$ clusters and of the KCl molecule. The vertical bars in the theoretical spectra correspond to the individual transitions of heights proportional to their K^{-2} $2h$ populations. Enhanced spectral features appearing due to the presence of chloride (green) and water (red) in the clusters are shown in the insets. The spectra are obtained by Gaussian convolution with a fwhm parameter of 3 eV. The $KCl(H_2O)_6$ cluster has a distinctive geometry, and its Auger spectrum should not be considered as a continuation of the series of the Auger spectra of the other calculated clusters.

We use the double ionization potential scale to compare experimental and theoretical results. The double ionization potentials of the clusters have been computed by means of a second order algebraic diagrammatic construction method, ADC(2),[20] which is an all-electron *ab initio* Green's function method. We used relativistic pseudopotental basis sets[21] augmented with diffuse and polarization functions for the heavy atoms. A double-ζ quality basis set[22] was chosen for the hydrogen atom. Note that the double ionization potentials are obtained directly without evaluating total energies of the initial and final states. The configuration space of the ADC(2) method comprises all the two-holes ($2h$) configurations and all their single excitations ($3h1p$) with respect to the Hartree−Fock ground state. It grows rapidly with the number of active electrons

(18) Berzinsh, U.; Gustafsson, M.; Hanstorp, D.; Klinkmüller, A.; Ljungblad, U.; Mårtensson-Pendrill, A.-M. *Phys. Rev. A* **1995**, *51*, 231.
(19) Olleta, A. C.; Lee, H. M.; Kim, K. S. *J. Chem. Phys.* **2007**, *126*, 144311.
(20) Schirmer, J.; Barth, A. *Z. Phys. A* **1984**, *317*, 267.
(21) Küchle, W.; Dolg, M.; Stoll, H.; Preuss, H. *Mol. Phys.* **1991**, *74*, 1245.
(22) Dunning, T. H., Jr. *J. Chem. Phys.* **1989**, *90*, 1007.

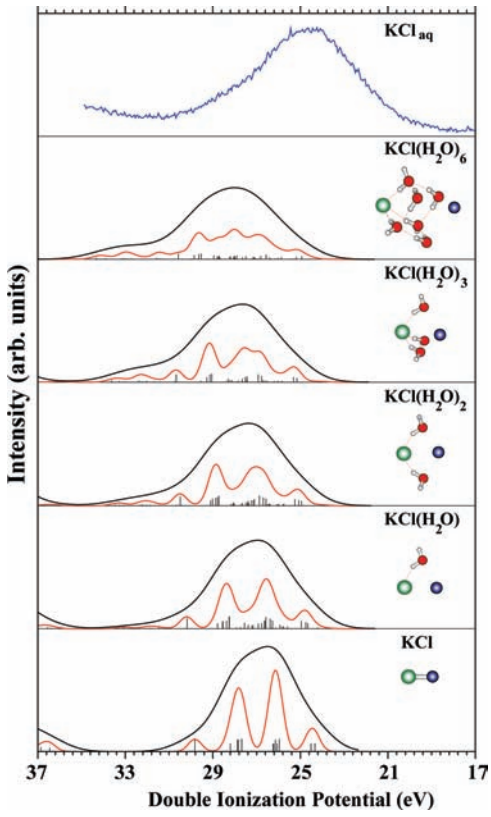

Figure 5. Comparison of the experimental Cl^- Auger spectrum of aqueous KCl with the calculated spectra of the $KCl(H_2O)_{1-3,6}$ clusters and of the KCl molecule. The vertical bars in the theoretical spectra correspond to the individual transitions of heights proportional to their Cl^{2-} 2*h* populations. The spectra are obtained by Gaussian convolution with a fwhm parameter of 3 eV (black) and 1 eV (red).

and functions in the basis sets used. Being, however, efficiently implemented by Tarantelli[23] with applications of modern integral-driven algorithms and procedures for diagonalization of the underlying large eigenvalue problem, the ADC(2) method is capable of treating systems with thousands of dicationic states which can hardly be handled by means of wave function methods with a similar level of correlation treatment.

The solution of the eigenvalue problem within the ADC(2) method yields, together with the double ionization potentials, also transition moments between the *N*-particle ground and *N* − 2-particle final states which are related to the spectral intensities. By using a two-hole population analysis[24] we represent the 2*h* part of the transition moments as a sum of various contributions characterized by different localizations of the final holes. In particular, we are able to distinguish between contributions where both final holes are localized on the same subunit, for example on potassium or chlorine, and the others where the final holes reside on different subunits, for example on potassium and water. In such a way, we get insight into characters of all the dicationic states under study. Only those contributions where both final holes reside on K^+ or Cl^- are used then to construct the theoretical Auger spectra shown below. The two-hole population analysis has been proven to be very useful for simulating essential features of the intensity distributions in the Auger spectra of various systems.[24−29] Additional details on the modeling of the theoretical Auger spectra of the clusters considered are given in Supporting Information.

K^+ Auger Spectra. In Figures 4 and 5, the experimental K^+ and Cl^- Auger spectra of aqueous KCl are shown together with the calculated spectra of the $KCl(H_2O)_n$ clusters and of the bare KCl molecule. The shapes of the theoretical spectra have been obtained by convoluting each computed transition by a Gaussian profile with a full width at half-maximum (fwhm) parameter of 3 eV that provides spectral shapes similar to those of the experimental spectra of aqueous KCl. The spectra of the KCl molecule were computed for calibration purposes to assess the impact of water. Furthermore, they helped us to estimate the accuracy of the ADC(2) method. By comparing the calculated electronic transition energies with the available experimental data for KCl, we found that ADC(2) overestimates double ionization potentials (DIP) by up to 1 eV. The experimental DIPs were deduced from the experimental K 2p photoelectron[30] and K^+ LMM Auger spectra[8] of the gas phase KCl molecule.

In the energy region considered, the K^+ Auger spectrum of the KCl molecule reveals the main feature comprising the final states which carry most of the Auger intensity. These are the K^{3+} $(3p)^{-2}$ Auger states where two outer valence electrons of K^+ are removed. This feature has much in common with the $L_{2,3}MM$ Auger spectrum of the Ar atom[31] except for the fact that the molecular field in KCl removes the degeneracy of the K^+ (3p) orbital and an energy splitting of the ^1D and ^3P Auger states thus occurs. The Gaussian convolution of the spectral lines gives rise to the intensity distribution seen in Figure 4 where the main feature exhibits two peaks and two shoulders. The most intense peak comprises the L_3MM (^3P) and L_2MM (^1D) Auger states while the other one bears its intensity due to the L_3MM (^1D) and L_2MM (^1S) Auger states. The L_2MM (^3P) and L_3MM (^1S) give rise to the low and high energy shoulders, respectively.

A second feature lies about 25 eV lower in energy than the main feature. Interatomic Auger processes lead to this feature which comprises the $(K^{2+}\ (3p)^{-1} + Cl(3p)^{-1})$ final states where two electrons are removed, one from each of the different K^+ and Cl^- sites. The high energy of the Auger electron is unfavorable for an efficient interatomic Auger decay.[32] As a rule, the rate of such a process is much lower and the intensity of the corresponding spectral feature is much weaker compared to those of the conventional intra-atomic Auger process. One may however encounter interatomic decay processes where the emitted electrons stem from molecular orbitals which have remarkable overlaps with the initially ionized subunit.[33]The corresponding transition rates are noticeably enhanced in these cases and the respective spectral features acquire remarkable intensity.

(23) Tarantelli, F. *Chem. Phys.* **2006**, *329*, 11.
(24) Tarantelli, F.; Sgamelloti, A.; Cederbaum, L. S. *J. Chem. Phys.* **1991**, *94*, 523.
(25) Minelli, D.; Tarantelli, F.; Sgamellotti, A.; Cederbaum, L. S. *J. Electron Spectrosc. Relat. Phenom.* **1995**, *74*, 1.
(26) Tarantelli, F.; Sgamellotti, A.; Cederbaum, L. S. *Phys. Rev. Lett.* **1994**, *72*, 428.
(27) Tarantelli, F.; Cederbaum, L. S. *Phys. Rev. Lett.* **1993**, *71*, 649.
(28) Feifel, R.; Eland, J. H. D.; Storchi, L.; Tarantelli, F. *J. Chem. Phys.* **2005**, *122*, 144309.
(29) Bolognesi, P.; Coreno, M.; Avaldi, L.; Storchi, L.; Tarantelli, F. *J. Chem. Phys.* **2006**, *125*, 054306.
(30) Pennanen, V.; Matila, T.; Kukk, E.; Huttula, M.; Aksela, H.; Aksela, S. In *MAX-Lab Activity Report 2000*; MAX-lab National Laboratory: Lund, Sweden, 2001; p 176.
(31) Werme, L. O.; Bergmark, T.; Siegbahn, K. *Phys. Scr.* **1973**, *8*, 149.
(32) Matthew, J. A. D.; Komninos, Y. *Surf. Sci.* **1975**, *53*, 716.
(33) Averbukh, V.; Müller, I. B.; Cederbaum, L. S. *Phys. Rev. Lett.* **2004**, *93*, 263002.

In the strongly bound ionic KCl molecule the outer valence molecular orbital Cl 3p overlaps considerably with those of potassium. As a consequence the respective interatomic Auger feature mentioned above shows up.

The addition of water molecules to KCl results in noticeable changes of the KCl Auger spectra. First of all, a new spectral feature arises in the K^+ Auger spectra of all the hydrated KCl clusters studied. It occupies nearly the same energy region from 40 to 50 eV in the Auger spectra of the $KCl(H_2O)_n$ ($n = 1-3$) clusters. In the spectrum of $KCl(H_2O)_6$ it appears at somewhat lower energy. This new spectral feature originates from those final states where one outer valence electron is removed from the potassium ion and another one from the water. The appearance of this feature in the Auger spectra is exciting by the unexpected fact that its intensity is comparable to that of the spectral feature attributed to the interatomic Auger process in the isolated KCl molecule. Note that the bonding between the potassium ion and the water molecules is substantially weaker than that between the K^+ and Cl^- ions in the isolated KCl molecule where a strong ionic bond is present.

The multicenter decay processes occurring in weakly bound systems have been attracting considerable attention from both theoreticians and experimentalists since the discovery of the interatomic (intermolecular) Coulombic decay (ICD), see ref 34 and refs 33, 35−37. ICD is primarily considered as an electronic decay of inner valence vacancies where it usually dominates over all possible relaxation mechanisms in the absence of an energetically forbidden Auger decay. However, ICD can also be operative in the core level regime where it may exert a remarkable influence on the electronic decay. This is expected in cases where orbital overlap between the constituents or neighbors is present. For instance, in the case of the not particularly deep Xe 4d core hole in the XeF_2 and XeF_4 clusters, ICD and related interatomic decay processes compete efficiently with the intra-atomic Auger decay while in the XeF_6 cluster the former processes dominate by far over the latter one.[38] Recently, experimental evidence of ICD following the O1s excitation in OH^- has been revealed in a NaOH aqueous solution.[39] ICD which involves water molecules surrounding the OH^- anion turns out to be the dominant decay process.

Although we did not fully analyze the precise multicenter decay mechanisms operative in weakly bound subunits of the microsolvated KCl clusters, we may assume that ICD is suited for describing such processes. This, first of all, refers to the processes occurring between each of the K^+ and Cl^- ions and the water molecules as well as between the ions themselves if they are separated from each other as in the case of the $KCl(H_2O)_6$ cluster. For brevity, we shall address the features in the K^+ Auger spectra which involve the electrons of Cl^- as the "chloride feature", and the features where the electrons of the water are involved as the "water feature".

As one can see in the spectra of the $KCl(H_2O)_{1-3}$ clusters, the intensities of both the water and the chloride features increase with the number of the water molecules, whereby the water feature grows faster. The intensity increase of the water feature is expectable and attributed to the increasing efficiency of the ICD processes due to the growing number of the available ICD channels upon the addition of the new water molecules.[40] In contrast, the intensity increase of the chloride feature is surprising since the distance between the counterions in the KCl molecule increases upon the sequential hydration (see Supporting Information) and the efficiency of the corresponding interatomic decay should be suppressed. We suggest that the water molecules play an important role in this decay process as well. The latter might be mediated by the water bridges whose outer valence orbitals have non-negligible overlaps with the counterions of the salt molecule.

In the $KCl(H_2O)_6$ cluster the large K−Cl distance and the double layered water cluster placed between the ions do not favor the electronic decay which involves the electrons of Cl^-, and therefore, the corresponding feature disappears in the Auger spectrum while the water feature remains. Interestingly, in the experimental spectrum of the KCl aqueous solution (see the upper panel of Figure 4) the chloride feature acquires considerably less intensity than the water feature. This may indicate that the KCl molecules in this solution undergo dissociation rather than represent contact ion pairs.

Note that the intensity of the water feature in the K^+ Auger spectrum of $KCl(H_2O)_6$ cluster is noticeably lower than that in the spectrum of the $KCl(H_2O)_3$ cluster although the number of the available ICD channels is considerably higher in the former case. The reason has mainly to do with an unfavorable orientation of the water molecules constituting the closest to the potassium ion water ring. The orbital overlap between these molecules and K^+ is small compared to that in $KCl(H_2O)_3$. The orbital overlap between K^+ and the water molecules from the farthest water ring is small because the species are simply far apart.

As a further impact of hydration, energy shifts of various electronic transitions in the K^+ Auger spectrum occur. We restrict, however, our consideration to the main feature experiencing the largest energy shift upon hydration. As one can see from Figure 4, the main feature in the spectrum of aqueous KCl exhibits a negative energy shift of about 9.5 eV with respect to that of the bare KCl molecule. The main feature in the spectra of the microsolvated $KCl(H_2O)_{1-3}$ clusters moves gradually to lower energies as the number of the water molecules grows. The $KCl(H_2O)_6$ cluster falls, however, out of the sequence by showing a reverse behavior of the main spectral feature.

Electrostatic and polarization interactions are expected to play a dominant role in the energy shifts of the main feature in the K^+ Auger spectrum when KCl dissolves in water. In order to derive precisely the impact of each interaction separately, an elaborative study is needed comprising, in particular, an analysis of the electronic density distributions in both the ground and doubly ionized states of the clusters studied. Such a study is beyond the scope of the present paper. Here, we only briefly mention the general trends resulting from the changes in the interaction picture due to growing cluster size.

(34) Cederbaum, L. S.; Zobeley, J.; Tarantelli, F. *Phys. Rev. Lett.* **1997**, *79*, 4778.
(35) Marburger, S.; Kugeler, O.; Hergenhahn, U.; Möller, T. *Phys. Rev. Lett.* **2003**, *90*, 203401.
(36) Jahnke, T.; Czasch, A.; Schöffler, M. S.; Schössler, S.; Knapp, A.; Käsz, M.; Titze, J.; Wimmer, C.; Kreidi, K.; Grisenti, R. E.; Staudte, A.; Jagutzki, O.; Hergenhahn, U.; Schmidt-Böcking, H.; Dörner, R. *Phys. Rev. Lett.* **2004**, *93*, 163401.
(37) Öhrwall, G.; Tchaplyguine, M.; Lundwall, M.; Feifel, R.; Bergersen, H.; Rander, T.; Lindblad, A.; Schulz, J.; Peredkov, S.; Barth, S.; Marburger, S.; Svensson, U. H. S.; Björneholm, O. *Phys. Rev. Lett.* **2004**, *93*, 173401.
(38) Buth, C.; Santra, R.; Cederbaum, L. S. *J. Chem. Phys.* **2003**, *119*, 10575.
(39) Aziz, E. F.; Ottosson, N.; Faubel, M.; Hertel, I. V.; Winter, B. *Nature* **2008**, *455*, 89–91.
(40) Santra, R.; Zobeley, J.; Cederbaum, L. S. *Phys. Rev. B* **2001**, *64*, 245104.

The double ionization threshold of the isolated K^+ is 77.4 eV.[10] In the free KCl molecule the presence of Cl^- stabilizes the triply ionized states of K stronger than the singly ionized states, thus reducing the double ionization potentials of K^+ compared to those of the isolated K^+ ion (see Figure 4). What happens when water molecules are added to KCl? First, the separation between K^+ and Cl^- increases with increasing the number of the water molecules in the clusters studied, and this gives rise to an increase of the double ionization potentials of K^+. Second, the electrostatic interaction of K^+ and K^{3+} with the dipoles of the water molecules and the polarization interaction come into play. Both K^+ and K^{3+} polarize the water molecules, but the polarization effect of the K^{3+} ion is, of course, stronger than that of K^+, and this leads to a decrease of the double ionization potentials. In the clusters studied, the dipoles of the water molecules are aligned in such a way that their electrostatic interaction with the K^+ and K^{3+} ions in the initial and final states, respectively, stabilizes the energies of these states. The stabilization of the latter states is apparently stronger than of the former ones, and thus, the double ionization potentials decrease. The polarization effect and the effect of the electrostatic charge−dipole interactions are expected to be nearly proportional to the number of the water molecules in the $KCl(H_2O)_{1-3}$ clusters considered where the K−O distances and the orientation of the water molecules are nearly the same. In clusters with nonequivalent water molecules, in particular where some waters are present in the second coordination shell of the potassium ion (a few such cases were considered but the results are not shown), polarization and charge−dipole interactions are obviously not proportional to the number of solvent molecules. The impact of the water molecules in the second coordination shell on the interaction picture is considerably smaller than that of the waters in the first coordination shell. The spectra of clusters with the same number of water molecules directly coordinated to K^+ are similar in appearance apart from small energy shifts attributed to a different number of water molecules in the second coordination shell, to slightly different K−Cl bond lengths and to rearrangements of the water molecules in the first coordination shell.

The interaction picture in the $KCl(H_2O)_6$ cluster considerably deviates from those in the $KCl(H_2O)_{1-3}$ clusters because of the different number of the water molecules, their separations from the ions, and their orientations. By comparing the energies of the main features in the spectra of the $KCl(H_2O)_{1-3,6}$ clusters and the KCl molecule, we conclude that the stretching of the K−Cl bond in these clusters is overcompensated by the impacts of the charge-dipole and the polarization interactions. In aqueous KCl one can expect stronger stabilization of the triply and singly ionized states compared to those of the small hydrated KCl clusters, in particular due to polarization of water leading to a further decrease of the double ionization potentials.

Cl^- Auger Spectra. Let us now discuss the Cl^- Auger spectra shown in Figure 5. In the energy region considered, the spectrum of the KCl molecule is composed of the Cl^+ $(3p)^{-2}$ Auger states with binding energies lying between 24 and 30 eV. These states constitute the main spectral feature. The Cl^+ $(3s)^{-1}(3p)^{-1}$ states in the Cl^- Auger spectrum arise at higher energies and are only partially displayed in Figure 5. The onset of these Auger states is seen at 36.4 eV.

The interatomic decay following Cl 2p ionization of KCl would lead to the (Cl $(3p)^{-1}$ + K^{2+} $(3p)^{-1}$) final states. These states have been identified in our calculations in the Cl^- Auger spectra of the KCl molecule and the hydrated KCl clusters. Their binding energies overlap energetically with the binding energies of the Cl^+ $(3s)^{-1}(3p)^{-1}$ Auger states in the spectrum of the KCl molecule that makes studies of such interatomic Auger states prohibitive from the experimental point of view unless coincidence measurements are performed. However, the overlap between the (Cl $(3p)^{-1}$ + K^{2+} $(3p)^{-1}$) and Cl^+ $(3s)^{-1}(3p)^{-1}$ states disappears gradually upon sequential hydration of KCl since the binding energies of the latter states increase with growing number of the water molecules, while the binding energies of the former states remain essentially constant. According to our analysis, in those systems where the two kinds of states overlap considerably, i.e., in isolated KCl and $KCl(H_2O)$, a remarkable mixing between these states occurs leading to a strong intensity redistribution in the Auger spectra.

The binding energies of the final ICD states where one electron is removed from the chloride anion and another from water arise in the same energy region as the binding energies of the Cl^+ $(3p)^{-2}$ Auger states. The ICD states manifest themselves in the calculated Cl^- Auger spectra of the microsolvated clusters as numerous additional lines which are not present in the respective spectrum of the KCl molecule. Each ICD state acquires its intensity by interacting with the Auger states, and as a consequence, a remarkable redistribution of the spectral intensity occurs upon hydration. This effect is better seen by the example of the more resolved spectra shown in Figure 5. One can clearly see how the well-defined multipeak structure of the Cl^- Auger spectrum of the KCl molecule gradually disappears and the spectra of the clusters start to resemble that of aqueous KCl. In the less resolved spectra, the effect of the presence of the ICD states mainly manifests itself in the appearance of a prominent shoulder on the high energy side of the main feature, which is also seen in the experimental spectrum of aqueous KCl.

As seen from Figure 5 the main features in the Cl^- Auger spectra of the isolated and aqueous KCl molecules are separated by a negative energy gap of about 2 eV. Surprisingly, in the spectra of the clusters studied, slight, but positive, energy shifts of the main features arise compared to the energy of the main feature in the spectrum of the isolated KCl molecule.

Let us briefly discuss the role of various interactions in the changes of the double ionization potentials of the Cl^- anion. In contrast to K^+, the double ionization potentials of the Cl^- anion increase in the presence of a counterion of an opposite sign and/or water molecules as the charge of Cl^- changes to its reverse after the double ionization. Note that the double ionization threshold of the isolated Cl^- is 16.6 eV which is far below the respective values in the systems studied here (see Figure 5). Since the electrostatic interaction of the resulting Cl^+ with K^+ and with the dipoles of the water molecules for the computed structures of the clusters are repulsive, the energies of the final states are destabilized. The polarization interaction does not play an important role in view of the independence of this interaction on the sign of the charge. When the number of water molecules around Cl^- grows in the clusters studied, the double ionization potentials of the anion grow as well, in particular, due to the growing charge−dipole interaction which overcompensates for the decrease in the double ionization potentials caused by the stretching of the K−Cl bond upon sequential hydration. To fully understand the energy shift in aqueous KCl on a microscopic level it would be necessary to study larger clusters, in particular, to study a complete solvation

shell around Cl^- and employ a plausible model for the long-range interaction.

Conclusion

In this paper, we have applied AES to study solvated ions. State-of-the-art calculations have been performed for microsolvated clusters to interpret the experimental results. The Auger spectrum of the K^+ ion clearly shows contributions from delocalized final states with vacancies on the surrounding water molecules. The situation for the Auger spectrum of the Cl^- ion is more complex, since final states localized on the core−hole site and delocalized states with vacancies on surrounding water molecules overlap in energy. The analysis of the populated final states has revealed that properties of these states depend strongly on the geometric and electronic structures of the local environment surrounding the unit with the initial core vacancy. This makes the spectroscopy described here a very promising tool to sensitively probe the solvent−solute interactions in aqueous solutions. With further development of the experimental measurements and the calculations, more information concerning the bonding could possibly be obtained from quantitative comparisons of theory and experiment.

Acknowledgment. The Royal Thai Government and Nakhon Phanom University are gratefully acknowledged for the graduate fellowship of W.P. This work has been financially supported by the Swedish Research Council (VR), the Göran Gustafsson foundation, the Knut and Alice Wallenberg foundation, the Foundation for International Cooperation in Research and Higher Education (STINT), the Foundation for Strategic Research (SSF), CNPq-Brazil, the Carl Tryggers Foundation, and the Deutsche Forschungsgemeinschaft. We also thank the MAX-lab staff for their helpful assistance during the experiments.

Supporting Information Available: Photoelectron spectra of the Cl^- 2p and K^+ 2p levels. Details of calculations concerning cluster geometries and double ionization spectra. This material is available free of charge via the Internet at http://pubs.acs.org.

JA8096866